Quantum Mechanical Study of Regioselectivity of Radical Additions to Substituted Olefins

ROGER ARNAUD,[1] VALENTINA VETERE,[2] VINCENZO BARONE[2]

[1]*Laboratoire d'Etudes Dynamiques et Structurales de la Sélectivité, Université Joseph Fourier, 301 Avenue de la Chimie, BP 53X, F-38041 Grenoble Cedex, France*

[2]*Dipartimento di Chimica, Università Federico II, Via Mezzocannone 4, I-80134 Napoli, Italy*

Received 12 November 1999; accepted 20 January 2000

ABSTRACT: Regiochemical trends in the addition of free radicals to substituted olefins are investigated by different quantum chemical approaches with special reference to oxygen centered radicals. From a methodological point of view, density functional methods provide correct general trends but they do not reach quantitative accuracy, especially for intermediate complexes. More reliable results are obtained by single point post-Hartree–Fock computations at density functional geometries. A number of test computations show that reoptimization of the geometry and computation of vibrational frequencies by correlated methods can be safely avoided. As a consequence, the overall computational approach has very reasonable computer costs. From a more chemical point of view, a careful analysis of computational results points out the significant role of anomeric and polar effects in tuning the common filicity of carbon centered radicals. J Comput Chem 21: 675–691, 2000

Keywords: radical additions; olefins; regiochemistry; anomeric and polar effects; density functional model; post-Hartree–Fock model

Introduction

Free radical additions to unsaturated substrates have received a great deal of attention because they play an important role in the synthesis of organic compounds, in biological mechanisms, and in polymerization processes. The factors controlling radical addition to multiple bonds have been carefully investigated[1, 2] and the importance of polar effects has been stressed. More recently, Fischer emphasized the role of the reaction enthalpy as a factor determining radical reactivity.[3]

As concerns the regiochemistry of the radical addition to unsymmetrical alkenes, the orientation of the attack was attributed to steric effects[1, 2] with the radical addition occurring on the less substituted carbon atom (hereafter referred to as the "regular," *r*, pathway). However, an "anomalous," *a*, pathway

Correspondence to: V. Barone; e-mail: enzo@chemna.dichi.unina.it

(preferential radical addition on the more substituted carbon atom) was experimentally observed in some cases; well known examples were provided by the preferential attack of methyl (Me) and fluoromethyl radicals at the CF_2 end of trifluoroethene. An anomalous regiochemistry was also established for the addition of the *tert*-butoxy (OtBu) radical to difluoro- and trifluoroethene,[4] the more fluorinated moiety being also more reactive toward OtBu.

Theoretical studies devoted to the addition of oxygen centered radicals to alkenes are scarce and concern the hydroxyl radical almost exclusively.[5–8] Previous *ab initio* calculations [unrestricted Hartree–Fock (UHF) 4-31G] on the methoxy (OMe) radical addition (taken as a model of the oxygen centered radical) to difluoro-1,1-ethene correctly reproduce the regiochemistry of the reaction,[9] but the level of calculation is not sufficient for quantitative predictions of reaction rates and exothermicities; in addition, the structures of weakly bonded intermediate adducts (*vide infra*) were not determined in this work. It was found that radical reactions are not easy to describe theoretically and generally post-HF models are needed to obtain reliable barriers for this class of reactions.[10] In the last decade much interest was shown in methods rooted in the Kohn–Sham (KS) approach to density functional theory (DFT)[11] and, more recently, to hybrid HF/KS methods,[12, 13] which are promising for the study of structures, spectroscopic properties, and reactivity of free radicals.[14–18] HF/KS studies of radical regioselectivity are less documented: two studies devoted to the attack of carbon centered radicals to unsymmetrical fluoroethenes seem to indicate that HF/KS approaches overestimate fluorine substituent effects.[19, 20] Because experimental data are available concerning the regiospecificity of *tert*-butoxy radical addition to fluoroethenes,[4] these systems constitute another interesting subject for a better understanding of the regioselectivity of radical addition to π bonds. In this work the addition of OMe and OtBu radicals to fluoroethene is studied by means of HF/KS and post-HF calculations in order to investigate in detail the potential energy surfaces associated with these systems, verify the reliability of the different computational models in reproducing experimental data, and discuss the factors influencing the regioselectivity of alkoxy radicals with special reference to the analogous reactions of carbon centered radicals.

In addition, we investigated the effect of radical polarity on the regiospecificity of the addition to a model substrate, 1,1-difluoroethene. To this end we considered CH_3 (neutral), CF_3, and CH_2CN (electrophilic), and CH_2OH (nucleophilic) radicals whose behavior was analyzed by the state correlation diagram (SCD) model.

Computational Details

All the computations are based on the unrestricted KS (UKS) approach to DF theory[11] as implemented in the Gaussian 98 package.[21] On the grounds of previous experience[14–20] we selected the so-called B3LYP hybrid functional that combines HP and Becke exchange terms with the Lee–Yang–Parr correlation functional in the same ratios as those optimized by Becke for a similar (although not identical) functional.[13] The geometries of reactants, prereaction complexes, transition states, and radical products were optimized and vibrational frequencies were calculated at the B3LYP/6-31G(d) level of theory.[22] The presence of prereaction complexes was established by tracing the intrinsic reaction coordinate.[23] Basis set truncation effects were further investigated by B3LYP single-point calculations using 6-311+G(2df,2p) (methoxy addition) or 6-311+G(d,p) (*tert*-butoxy addition) basis sets.[22] Additional post-HF calculations were made with projected second-order Møller–Plesset (PMP2) and quadratic configuration interaction single double (QCISD) methods.[22]

Canonical rate constants were computed using the conventional transition state (TS) theory, whose results can be formally rewritten in terms of pseudothermodynamic functions[24]

$$k(T) = \chi \frac{KT}{h} R' T^{-\Delta n} \exp\left(\frac{\Delta S^{\neq}}{R}\right) \exp\left(\frac{-\Delta H^{\neq}}{RT}\right). \quad (1)$$

In this equation the χ is the transmission coefficient (taken in the following as unitary), K is the Boltzmann constant, T is the absolute temperature, h is Planck's constant, Δn is the variation in the number of particles in going to the TS (-1 for bimolecular reactions), $\Delta H^{\neq}$ and $\Delta S^{\neq}$ are the enthalpy and entropy changes between reactants and the transition structure, R is the ideal gas constant (in units coherent with those used for $\Delta H^{\neq}$ and $\Delta S^{\neq}$), and R' has the same meaning but in l atm^{-1} (0.082).

A quantitative analysis of anomeric effects (*vide infra*) can be obtained using the Fock matrix deletion approach based on the so-called natural bond orbitals.[25] Although this procedure is not self-consistent, the error in the energy is negligible as long as the interactions that were dropped from the Fock matrix are not strongly coupled with other

interactions.[26] For open-shell systems, elements of the α and β Fock matrices can be deleted independently.

Possible hydrogen bonds formed in different stages of the reactions were characterized by means of the atoms in molecules (AIM) theory of Bader.[27] Previous studies indicated that for hydrogen bonds the charge density ρ_C should be low and the Laplacian of the charge density $\nabla^2\rho_C$ positive[28] with a good linear correlation between ρ_C and the strength of the interaction.[29]

Results and Discussion

In the following text the bold face letters represent the attacked site of the fluoroethenes; prereaction complexes, TSs, and radical products will be referred to as **C**, **TS**, and **P**, respectively. This is illustrated in Figure 1 together with a schematic reaction path.

OPTIMIZED STRUCTURES

Prereaction Complexes

The IRC calculations indicate that, for all the systems, the TSs are connected to prereaction complexes, which are depicted in Figure 2.

In the OMe addition reactions only one structure was found for both directions of the attack, showing that the reaction bifurcates into two different pathways after the formation of the complex. A similar situation was observed for the addition of a hydroxyl radical to monohaloethenes.[8] The OtBu approach to trifluoroethene leads to the formation of only one association, while two different stable structures could be characterized for the addition to the mono- and difluoroethene. In both cases reactant moieties are only slightly distorted. Inspection of Figure 1 shows that these intermediates are reached for two different orientations of the alkoxy radical with respect to the substrate: either the O—C and C=C bonds are almost orthogonal [e.g., **C** (OMe, CH_2CF_2) or **C** (OtBu, $CH_2\mathbf{CF_2}$)] or these two bonds are almost parallel [e.g., **C** (OMe, CH_2CHF) or **C** (OtBu, $\mathbf{CH_2}CF_2$)]; this latter orientation gives rise to a shortening of the distances between fluorine and hydrogen atoms of the radical. The equilibrium structures of the prereaction complexes seem to be determined by a balance between two kinds of weak interactions: an electron density delocalization (from an oxygen lone pair, LP_O, into the antibonding π^*_{CC} orbital of fluoroethene and from the occupied β-π_{CC} spin orbital into the vacant β-LP^*_O spin orbital) and an unconventional C—H···F intermolecular hydrogen bond. The main characteristics of these interactions are summarized in Table I.

In **C** (OMe, CH_2CF_2) and **C** (OtBu, $CH_2\mathbf{CF_2}$) the radical is shifted toward the CF_2 terminus, thus allowing an additional $LP_O \rightarrow \sigma^*_{CF}$ delocalization to occur (-4.2 and -1.9 kJ mol^{-1}, respectively). The "orthogonal orientation" maximizes the stabilizing delocalization interactions. In a general way, delocalization energies are less stabilizing in OtBu complexes while OtBu is more able than OMe to give C—H···F hydrogen bonds. Insofar as the relative orientation of reactant molecules results from a delicate balance between these two interactions, it is natural to observe structural differences in the prereaction complexes. However, these differences do not predetermine the TS geometries.

Radical Products

The most stable conformers resulting from different orientations of the radical O—C bond with respect to the fuoroethenes are shown in Figures 3

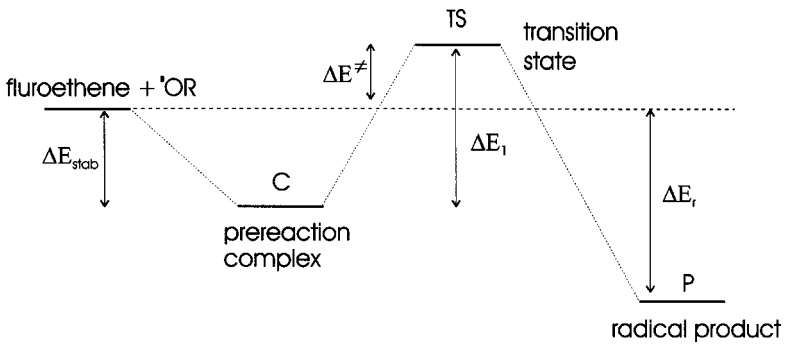

FIGURE 1. An energetic diagram for radical additions to ethenes.

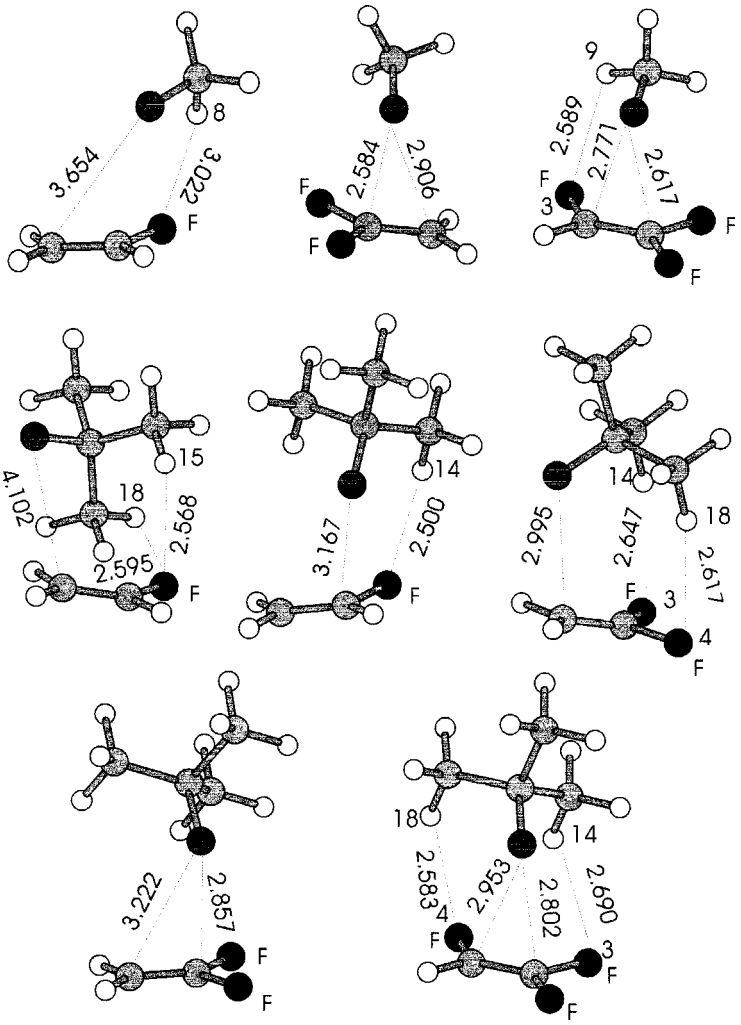

FIGURE 2. Structures and atom numbering of prereaction complexes.

TABLE I.
Natural Bond Orbital Charge Transfer and Hydrogen Bond Critical Points (CP) Analysis in Prereaction Complexes from B3LYP/6-31G(d) Computations.

Complex	$LP_O \rightarrow \pi^*_{CC}$	$\pi_{CC} \rightarrow LP^*_O$	Location of CP	ρ_C	$\nabla^2\rho_C$
C (OMe, CH_2CHF)	−1.9	−1.4	$F\cdots H_8$	0.0103	0.0147
C (OMe, CH_2CF_2)	−6.4	−8.6	None		
C (OMe, $CHFCF_2$)	−5.8	−13.1	$F_3\cdots H_9$	0.0067	0.0318
C (OtBu, $\mathbf{CH_2}CHF$)	0.0	0.0	$F_6\cdots H_{15}$	0.0061	0.0275
			$F_6\cdots H_{18}$	0.0057	0.0260
C (OtBu, $CH_2\mathbf{CHF}$)	−0.8	−1.1	$F\cdots H_{14}$	0.0073	0.0317
C (OtBu, $\mathbf{CH_2}CF_2$)	0.0	0.0	$F_3\cdots H_{14}$	0.0055	0.0253
			$F_4\cdots H_{18}$	0.0051	0.0264
C (OtBu, $CH_2\mathbf{CF_2}$)	−3.9	−2.5	None		
C (OtBu, $CHFCF_2$)	−3.0	−5.3	$F_3\cdots H_{14}$	0.0044	0.0219
			$F_4\cdots H_{18}$	0.0061	0.0283
			$F_4\cdots H_{188}$	0.0052	0.0252

The atom numbering is given in Figure 2. Delocalization energies are in kilojoules per mole (kJ mol^{-1}).

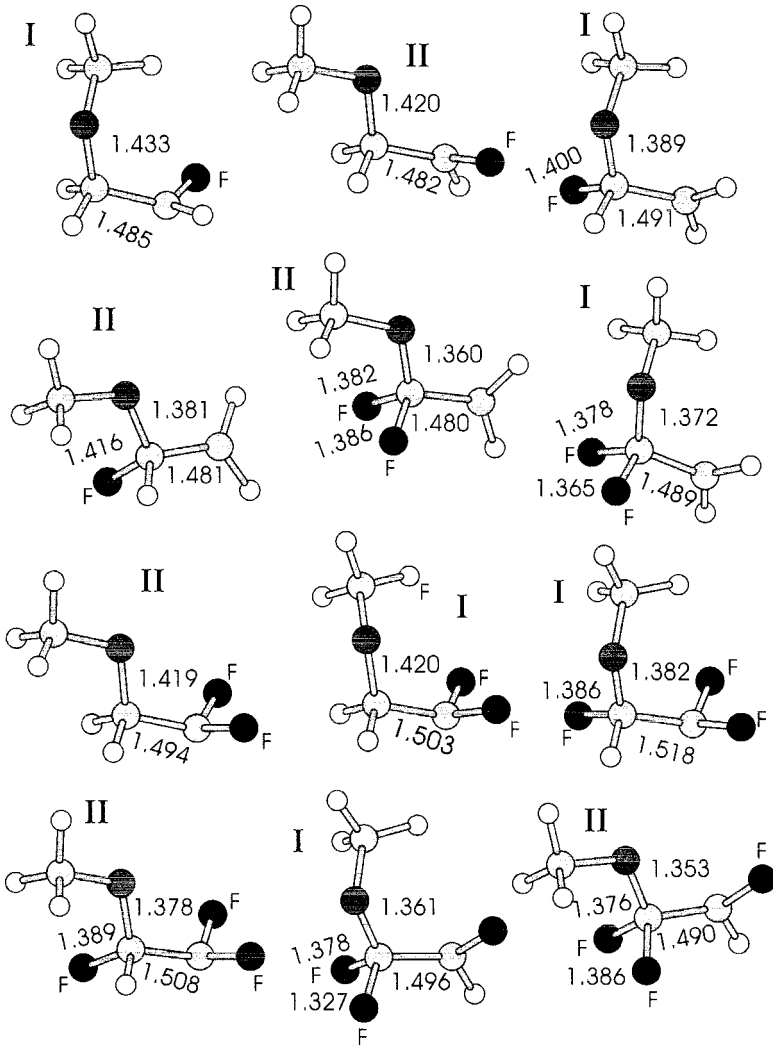

FIGURE 3. Structures of product radicals issuing from the addition of OMe to fluorinated ethenes.

and 4 and their relative stabilities are given in Table II.

In all cases the third staggered conformer (not given in Table II or in the figures) is considerably less stable. As mentioned previously,[30] a large $LP_O \rightarrow \sigma^*_{CF}$ delocalization energy is found for the gauche conformers of radical products resulting from the addition on substituted carbon atoms of fluoroethene. The trend of C—O bond lengths is parallel to that of the delocalization energies: the largest $LP_O \rightarrow \sigma^*_{CF}$ stabilizing interaction corresponds to the shortest C—O bond: e.g., a delocalization energy of -118.4 kJ mol^{-1} [**P** (OMe, CHF**CF$_2$**)] is associated with a C—O distance of 1.353 Å whereas the corresponding values in **P** (OMe, **CH$_2$**CHF) are -20.7 kJ mol^{-1} and 1.433 Å, respectively. At the same time, partial occupation of the antibonding σ^*_{CF} orbitals leads to a lengthening of the C—F bonds. When the addition occurs at a substituted end (CHF or CF_2) of the substrate, conformers II are always the most stable and involve the largest delocalization energies. For radical products resulting from the addition on the unsubstituted carbon atom, conformers I (see Figs. 3, 4) are the most stable, despite the fact that weak delocalization energies should favor conformers II. We were not able to locate any bond critical point between hydrogen atoms of the methoxy radical and F atoms of the fluoroethene substrates. On the other hand, the AIM analysis revealed the presence of weak hydrogen bonds in all **P** (OtBu, fluoroethenes). However, the weak values of the charge density ρ_C at the bond critical points (Table II) seemed to indicate that these interactions do not play a significant role in determining the preferred conformations of the products. (In particular, no relationship was established between the

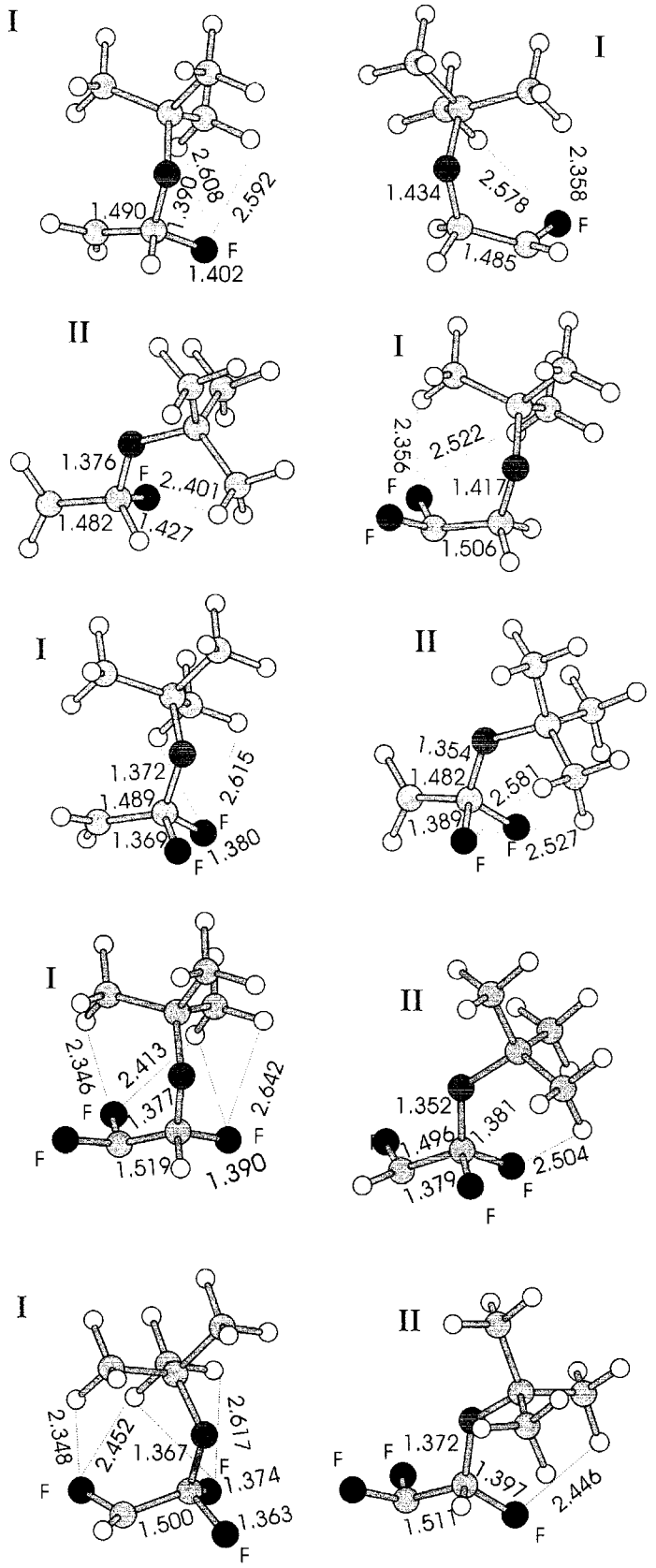

FIGURE 4. Structures of product radicals issuing from the addition of OtBu to fluorinated ethenes.

TABLE II.

Relative Stabilities, ΔE (kJ mol^{-1}), of Conformers for Radical Products and Analysis of Intramolecular Delocalization and Hydrogen Bonding Interactions.

	OCH_3											
	CH_2CHF		CH_2**CHF**		**CH_2**CF_2		CH_2**CF_2**		**CHF**CF_2		CHF**CF_2**	
	I	II	I	II	I	II	I	II	I	II	I	II
ΔE	0.0	5.6	4.8	0.0	0.0	4.9	11.8	0.0	1.7	0.0	4.4	0.0
$LP_O \rightarrow \sigma^*_{CX}$	−20.7	−25.8	−67.7	−71.4	−21.0	−25.9	−83.5	−112.9	−67.0	−71.8	−98.5	−118.4
	$OC(CH_3)_3$											
ΔE			12.0	0.0			17.1	0.0	4.7	0.0	11.0	0.0
$LP_O \rightarrow \sigma^*_{CX}$	−19.1		−62.0	−80.1	−19.4		−78.6	−113.6	−75.6	−82.7	−90.2	−116.0
									0.0105		0.0111	
ρ_C	0.0107		0.0107	0.0106	0.0074		0.0108	0.0110	0.0093	0.0108	0.0085	0.0098
	0.0065				0.0107			0.0108	0.0110		0.0110	

All the computations were performed at the B3LYP/6-31G(d) level.

Delocalization is from the oxygen lone pair to the CXs antibonding orbital at the attacked carbon atom, $LP_O \rightarrow \sigma^*_{CX}$ (kJ mol^{-1}); the charge density is at the C—H···F bond critical point (ρ_C). The H···F bonds are given in Figure 4.

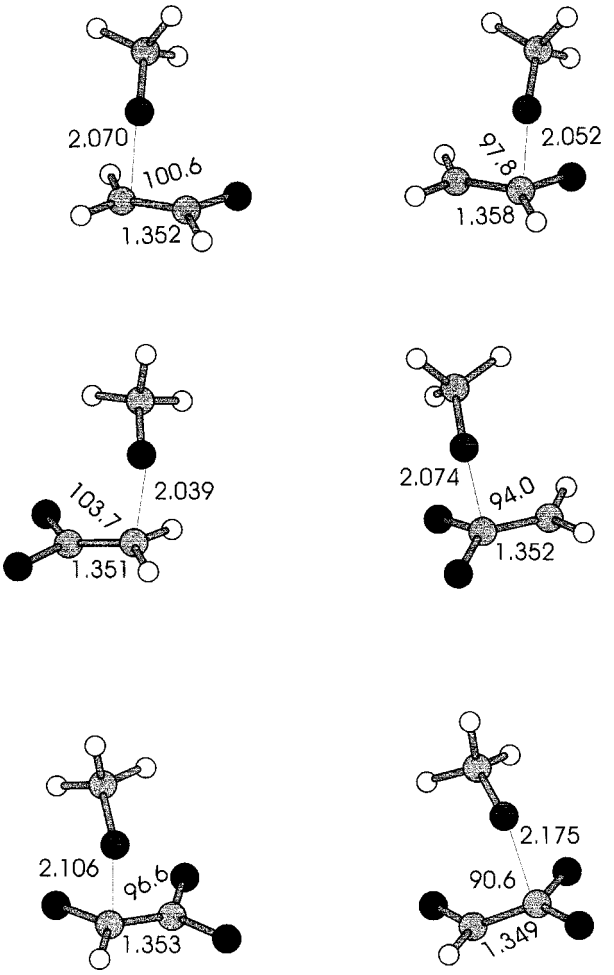

FIGURE 5. Structures of transition states governing the addition of OMe to fluorinated ethenes.

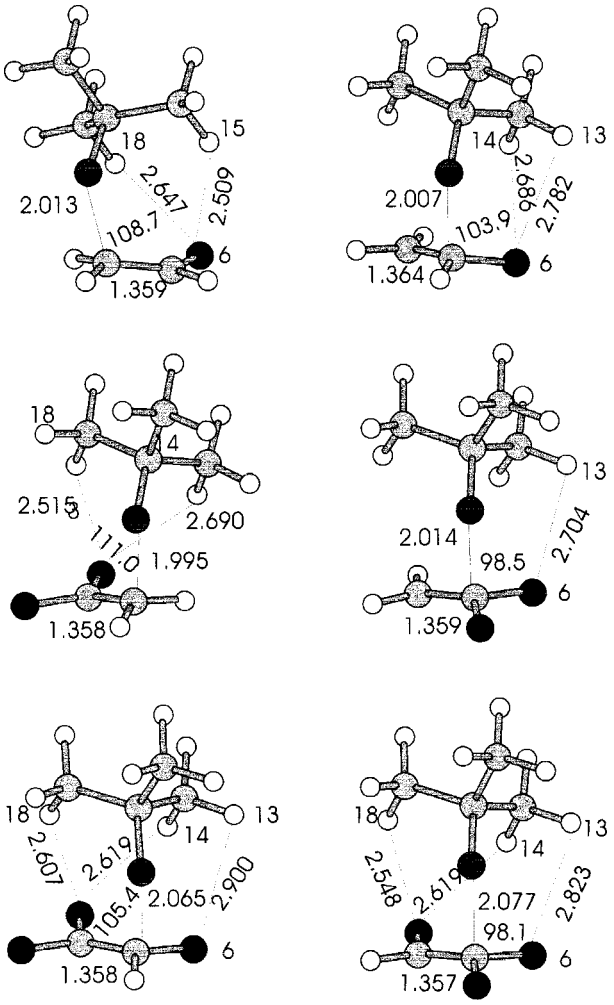

FIGURE 6. Structures of transition states governing the addition of OtBu to fluorinated ethenes.

strength of the hydrogen bonds and the relative stabilities ΔE.)

TSs

The TSs are sketched in Figures 5 and 6. Some supplementary structural information is given in Table III.

In the OMe series the TSs are reached for a dihedral angle $COC_{att}C$ of about 80° and for an intermolecular distance $O\cdots C_{att}$ increasing from 2.039 ($\mathbf{CH_2}CF_2$) to 2.175 Å ($CH_2\mathbf{CF_2}$). The corresponding values in the OtBu series are, respectively, 60°, 1.995 Å ($\mathbf{CH_2}CF_2$), and 2.077 Å ($CH_2\mathbf{CF_2}$). Furthermore, the COC_{att} angle is significantly larger when OtBu is the incoming radical (about 120° vs. 100°), which is probably due to larger steric hindrances. Geometrical data, as well as charge densities at the $O\cdots C_{att}$ bond critical points (see Table III), indicate that the formation of this bond is more advanced for OtBu additions with corresponding larger deformations of the fragments [as exemplified by the values of $\Delta r'$, $\Delta\Phi$, and $E_{def}(S)$]. Another point of interest is the variation of geometrical parameters and deformation energies with the regiochemistry of the addition reactions. It is noteworthy for all TSs that a smaller value of both $\Delta\Phi$ and $E_{def}(R)$ corresponds, for a given substrate, to the addition on the more substituted carbon atom. At the same time, the difference $\Delta(\Delta r') = \Delta r'$ (anomalous pathway) $- \Delta r'$ (regular pathway) decreases or becomes even negative, increasing the number of fluorine atoms in the substrate. As a result, comparable values of $E_{def}(S)$ are obtained for the different situations contrary to what was previously found for CH_3 additions to the same substrates [the CH_3 $E_{def}(S)$ is larger for the attack to the less substituted carbon atom by 5.9 (CH_2CHF), 12.6 (CH_2CF_2), and 5.3 ($CHFCF_2$)

TABLE III.
Geometric Parameters and Deformation Energies, E_{def} (kJ mol^{-1}), in Transition States (TSs) from B3LYP/6-31G(d) Computations.

	Δr[a]	$\Delta r'$[b]	$\Delta\Phi$[c]	$\rho_C(O\cdots C_{att})$	$E_{def}(S)$[d]	$E_{def}(R)$[d]
TS (OMe, **CH_2**CHF)	0.022	0.027	2.6	0.0595	7.3	1.7
TS (OMe, CH_2**CHF**)	0.024	0.033	2.6	0.0619	10.9	1.2
TS (OMe, **CH_2**CF_2)	0.023	0.029	4.0	0.0649	9.3	1.7
TS (OMe, CH_2**CF_2**)	0.021	0.030	2.6	0.0591	13.1	0.9
TS (OMe, **CHF**CF_2)	0.022	0.026	2.7	0.0577	13.6	1.3
TS (OMe, CHF**CF_2**)	0.018	0.022	1.7	0.0488	12.6	1.2
TS (OtBu, **CH_2**CHF)	0.027	0.034	2.6	0.0661	11.9	2.5
TS (OtBu, CH_2**CHF**)	0.026	0.037	2.6	0.0666	15.9	2.4
TS (OtBu, **CH_2**CF_2)	0.028	0.036	4.0	0.0701	13.6	2.6
TS (OtBu, CH_2**CF_2**)	0.025	0.036	2.6	0.0661	20.4	2.0
TS (OtBu, **CHF**CF_2)	0.026	0.032	2.7	0.0614	17.7	2.1
TS (OtBu, CHF**CF_2**)	0.024	0.031	1.7	0.0587	19.9	1.6

Distances are in angstroms and angles are in degrees.
[a] $\Delta r = d_{O—C}(TS) - d_{O—C}(radical)$.
[b] $\Delta r' = d_{C=C}(TS) - d_{C=C}(fluoroethene)$.
[c] $\Delta\Phi = 360°$ minus the sum of the three valence angles around the C_{att} center.
[d] For the fragment X (X = radical R or substrate S) $E_{def}(X) = E_{TS}(X) - E_0(X)$ where E_{TS} and E_0 are the energies computed using geometries optimized for the TSs and the reactants, respectively.

kJ mol^{-1}].[20] In our opinion this trend reflects the variations of the exothermicity (*vide infra*).

In all the TSs the O—C bond of the alkoxy radical is oriented, with respect to the C=C double bond, from the same side as the C—F bond. Two factors would explain the preference of a gauche rather than an anti conformation: the increased role of the stabilizing $LP_O \rightarrow \sigma^*_{Catt\text{-}F}$ delocalization interaction mentioned in the preceding paragraph, and the presence of weak intermolecular hydrogen bond interactions. Indeed, we have evidenced in Figures 4 and 5 some relatively short H···F distances, which might be diagnostic of such interactions.

The $LP_O \rightarrow \sigma^*_{Catt\text{-}X}$ (X = H, F) interaction energies were calculated using the NBO deletion procedure and the presence of weak C—H···F—C_{att} hydrogen bonds tested by the AIM population analysis. The results are collected in Table IV.

As expected, $LP_O \rightarrow \sigma^*_{Catt\text{-}F}$ delocalization energies are quite important and thus a part of the anomeric effect is already present in the TSs. Except for **TS** (OMe, **CH_2**CHF), hydrogen bonds are not found in TSs with OMe whereas their presence seems confirmed for all the TSs involving the OtBu radical. However, also in the latter case the role of H-bond interactions in determining the regiochemistry of the addition reaction should be weak, because they are comparable in all the TSs.

A rough estimate of hydrogen bond strengths can be obtained from the energy difference between **TS** (OMe, **CH_2**CHF) structures corresponding to the OMe radical on the same or on the opposite side of the F atom with respect to the C—O—C—C plane. The energy difference between these two structures is 3 kJ mol^{-1} at the B3LYP/6-31G(d) level and 4.3 kJ mol^{-1} at the PMP2/6-311+G(2d,2p)//B3LYP/6-31G(d) level. The same approach can be used for an estimation of the net oxygen LP delocalization (delocalization to $\sigma^*_{C—F}$ minus delocalization to $\sigma^*_{C—H}$) starting from **TS** (OMe, CH_2**CHF**); an energy difference of 5.6 kJ mol^{-1} is calculated at the B3LYP/6-31G(d) level, which is reduced to 4.6 kJ mol^{-1} at the PMP2/6-311+G(2d,2p)//B3LYP/6-31G(d) level.

We conclude this section by pointing out that the results of the AIM analysis do not automatically correlate with the geometrical features of the TSs: in particular, the highest ρ_C value does not always correspond to the shortest C—H···F distance. Thus, the AIM analysis does not reveal any critical point for **TS** (OMe, CH_2**CHF**), which is characterized by a short H···F distance (2.419 Å) whereas a critical point is found in **TS** (OMe,**CH_2**CHF) between F and H atoms that are 2.631 Å apart.

TABLE IV.
Natural Bond Orbital Charge Transfer and Hydrogen Bond Critical Points (CP) Analysis in Transition States (TS) from B3LYYP/6-31G(d) Computations.

TS	LPO $\rightarrow \pi^*_{CX}$	Location of CP	ρ_C	$\nabla^2\rho_C$
TS (OMe, $\mathbf{CH_2}$CHF)	−1.6	$F\cdots H_{10}$	0.0061	0.0295
TS (OMe, $CH_2\mathbf{CHF}$)	−5.8	None		
TS (OMe, $\mathbf{CH_2}CF_2$)	−2.2	None		
TS (OMe, $CH_2\mathbf{CF_2}$)	−13.3	None		
TS (OMe, $\mathbf{CHF}CF_2$)	−4.3	None		
TS (OMe, $CHF\mathbf{CF_2}$)	−9.1	None		
TS (OtBu, $\mathbf{CH_2}$CHF)	−2.7	$F_6\cdots H_{15}$	0.0076	0.0347
		$F_6\cdots H_{18}$	0.0054	0.0259
TS (OtBu, $CH_2\mathbf{CHF}$)	−8.8	$F_6\cdots H_{13}(H_{14})$	0.0079	0.0365
TS (OtBu, $\mathbf{CH_2}CF_2$)	−3.2	$F_3\cdots H_{14}$	0.0049	0.0238
		$F_3\cdots H_{18}$	0.0074	0.0340
TS (OtBu, $CH_2\mathbf{CF_2}$)	−14.9	$F_6\cdots H_{12}(H_{13})$	0.0073	0.0354
TS (OtBu, $\mathbf{CHF}CF_2$)	−7.2	$F_3\cdots H_{14}(H_{18})$	0.0069	0.0331
		$F_6\cdots H_{13}(H_{14})$	0.0056	0.0267
TS (OtBu, $CHF\mathbf{CF_2}$)	−12.6	$F_6\cdots H_{13}(H_{14})$	0.0070	0.0337
		$F_3\cdots H_{14}$	0.0059	0.0281
		$F_3\cdots H_{18}$	0.0068	0.0319

The atom numbering is given in Figure 2. Delocalization energies are in kilojoules per mole (kJ mol^{-1}).

ENERGETICS

Stabilization Energy of Prereaction Complexes

Stabilization energies are given in Table V; they are very sensitive to the level of theory and basis set employed.

The B3LYP method underestimates stabilization energies with respect to PMP2 results, except in the case of **C** (OMe, $CHFCF_2$), and the two approaches give conflicting results for the relative stabilization energies. Furthermore, any increase of the basis set size leads to a decrease of the stabilization energy, this effect being especially important at the B3LYP level. The inclusion of non-potential energy terms reduces the stability of the complexes; however, the existence of such associations seems well established, especially in the case of trifluoroethene. This point is noteworthy because the existence of an association between an alkoxy radical and trifluoroethene can explain the small negative energy barriers obtained with this substrate (*vide infra*).

Barrier Heights and Kinetic Parameters

All the results are collected in Table VI. Figure 1 shows the energetic diagram of investigated radical addition reactions.

We discuss first the energy barriers $\Delta E^{\neq}$. As far as the OMe addition is concerned, in agreement with previous calculations,[17, 18, 20] the $\Delta E^{\neq}$ values calculated at the B3LYP/6-31G(d) level are the lowest ones and this is also true for the ΔE_1 term defined Figure 6. The use of larger basis sets dramatically increases B3LYP barrier heights, which become larger than their PMP2 counterparts. Surprisingly, for the OtBu addition reactions B3LYP/6-31G(d) $\Delta E^{\neq}$ are higher than the PMP2/6-31G(d) ones. In the light of our results it seems very difficult to compare the reactivity of the two alkoxy radicals toward fluoroethenes. However, for a given radical, the predicted relative reactivity is the same: on the basis of $\Delta E^{\neq}$ values, trifluoroethene is the most reactive substrate.

The main topic of this study is the regiochemistry of the radical reactions and now we focus our attention on the energy difference $\Delta(\Delta E^{\neq}) = \Delta E^{\neq}(a) - \Delta E^{\neq}(r)$ (values in parentheses in Table VI). In every case, all the computational models give the same predictions: both radicals add preferentially to the unsubstituted carbon atom of CH_2CHF while the attack at the most substituted carbon atom is preferred in the case of di- and trifluoroethenes. Our results indicate that the OMe radical shows a lower selectivity between the carbon atoms of monofluo-

TABLE V.
Stabilization Energies (kJ mol^{-1}) of Prereaction Complexes.

	OMe		
Level	CH_2CHF	CH_2CF_2	$CHFCF_2$
B3LYP/6-31G(d)	−10.6	−8.2	−14.6
B3LYP/6-311+G(2d,2p)	−3.3	−1.2	−4.0
PMP2/6-31G(d)	−12.7	−9.4	−12.2
PMP2/6-311+G(2d,2p)	−9.6	−8.4	−10.6
Δ(ZPE)	3.0	4.1	5.1
ΔH_{stab}[a]	−7.3	−1.4	−12.3

	OtBu				
Level	$\mathbf{CH_2}CHF$	$CH_2\mathbf{CHF}$	$\mathbf{CH_2}CF_2$	$CH_2\mathbf{CF_2}$	$CHFCF_2$
B3LYP/6-31G(d)	−11.1	−10.7	−8.9	−7.4	−10.9
B3LYP/6-311+G(d,p)	−1.6	−2.4	−0.5	0.5	−2.4
PMP2/6-31G(d)	−14.3	−16.2	−14.9	−12.4	−21.8
PMP2/6-311+G(d,p)	−12.0	−15.1	−14.1	−12.6	−20.7
Δ(ZPE)	0.9	0.8	2.7	2.0	3.2
ΔH_{stab}[a]	−7.8	−4.6	−1.9	−3.4	−8.9

[a] Calculated at 333 K using the B3LYP/6-31G(d) level.

TABLE VI.
Barrier Heights, $\Delta E^{\neq}$ (kJ mol^{-1}), and Kinetics Parameters of Alkoxy Radical Addition to Fluoroethenes.

	OMe					
Level	$\mathbf{CH_2}CHF$	$CH_2\mathbf{CHF}$	$\mathbf{CH_2}CF_2$	$CH_2\mathbf{CF_2}$	$\mathbf{CHF}CF_2$	$CHF\mathbf{CF_2}$
$\Delta E^{\neq}$ [B3LYP/6-31G(d)]	2.3	2.5 (0.2)	5.4	0.4 (−5.0)	−6.7	−11.8 (−5.1)
$\Delta E^{\neq}$ [B3LYP/6-311+G(2d,2p)]	11.7	14.0 (2.3)	13.3	12.0 (−1.3)	5.5	1.9 (−3.6)
$\Delta E^{\neq}$ [PMP2/6-31G(d)]	7.8	8.9 (1.1)	15.1	10.3 (−4.8)	5.0	0.3 (−4.7)
$\Delta E^{\neq}$ [PMP2/6-311+G(2d,2p)]	9.2	9.3 (0.1)	13.5	10.4 (−3.1)	5.9	2.0 (−3.9)
Δ(ZPE) (kJ mol^{-1})	8.0	7.3	7.7	6.2	6.8	6.0
$\Delta H^{\neq}$[a] (kJ mol^{-1})	8.3	8.1	11.9	5.3	−6.0	−11.9
$\Delta S^{\neq}$ (kJ mol^{-1} K^{-1})	−154.9	−158.9	−147.5	−156.2	−154.9	−156.5
k_a/k_r	0.66		3.8		6.9	

	OtBu					
Level	$\mathbf{CH_2}CHF$	$CH_2\mathbf{CHF}$	$\mathbf{CH_2}CF_2$	$CH_2\mathbf{CF_2}$	$\mathbf{CHF}CF_2$	$CHF\mathbf{CF_2}$
$\Delta E^{\neq}$ [B3LYP/6-31G(d)]	9.6	13.6 (4.0)	13.5	10.6 (−2.9)	6.5	0.0 (−6.5)
$\Delta E^{\neq}$ [B3LYP/6-311+G(d,p)]	23.2	27.0 (3.8)	24.8	24.1 (−0.7)	17.8	13.6 (−4.2)
$\Delta E^{\neq}$ [PMP2/6-31G(d)]	5.7	9.2 (3.5)	12.5	10.7 (−1.8)	2.8	−2.5 (−5.3)
$\Delta E^{\neq}$ [PMP2/6-311+G(d,p)]	9.4	12.3 (2.9)	16.2	14.8 (−1.4)	6.5	2.7 (−3.8)
Δ(ZPE) (kJ mol^{-1})	5.0	3.6	5.3	3.0	4.3	3.8
$\Delta H^{\neq}$[a] (kJ mol^{-1})	14.7	17.6	18.8	13.7	5.2	−2.1
$\Delta S^{\neq}$ (kJ mol^{-1} K^{-1})	−163.5	−163.6	−152.8	−158.9	−170.1	−178.2
k_a/k_r	0.66 (0.36)[b]		3.0 (4.0)[b]		5.3 (4.5)[b]	

The values in parentheses are the differences between the barrier heights governing anomalous and regular pathways.
[a] Calculated from $\Delta E^{\neq}$ [B3LYP/6-31G(d)].
[b] Experimental value (ref. 4).

roethene than OtBu. This is quite surprising insofar as the presence in the **TS** (OMe, $\mathbf{CH_2}$CHF) of a weak hydrogen bonding exerts a stabilizing effect (see Table IV). For the alkoxy radicals addition to di- and trifluoroethene, the largest $|\Delta(\Delta E^{\neq})|$ are obtained from B3LYP/6-31G(d) calculations; in our recent study of the regiochemistry of the addition reaction of a methyl radical to trifluoroethylene, we established an opposite trend: the easiness of the anomalous pathway was underestimated with respect to post-HF procedures.[20] Hence, the B3LYP model does not fail systematically in predicting the regioselectivity of radical additions to multiple bonds. As mentioned previously, the presence of weak hydrogen bonding in OtBu TSs does not induce important differences in the regiospecificity of the two radicals. From this point of view OMe can be considered a good model for OtBu.

Turning next to nonpotential energy terms, it appears that zero point energy (ZPE) corrections raise the barriers and favor addition to the substituted end of fluoroethene, but thermal corrections offset the ZPE effect completely ($CHFCF_2$) or partially (CH_2CHF and CH_2CF_2). The calculated regiospecificities k_a/k_r corresponding to the addition of OtBu are in good agreement with the experimental data.

Reaction Energies and Reaction Enthalpies

These values are collected in Table VII. As mentioned by us[18, 20] and others,[8, 17] B3LYP reaction energies are too low with respect to post-HF calculations; this is also true for the difference in reaction energies of $\Delta E_r(a) - \Delta E_r(r)$.

At both levels a less exothermic process is predicted when the basis set is increased. The addition of nonpotential energy terms leads to larger $\Delta(\Delta H_r)$. A less exothermic addition is predicted for OtBu than for OMe. According to the Hammond postulate, this result is in line with the shorter intermolecular $O\cdots C_{att}$ distances in the TSs governing OtBu additions.

The stability difference between the radical products is a key factor in determining the regioselectivity.[31] Our results unambiguously show that the strengths of the O—C bond being formed are in the order O—CF_2 > O—CHF > O—CH_2. In a previous paragraph we discussed the role played by anomeric effects in determining the preferred conformations of the products. A quantitative analysis of such effects shows (see Table IV) that the $LP_O \rightarrow \sigma^*_{C—F}$ delocalization energy is ≈50 kJ mol^{-1} more stabilizing than the $LP_O \rightarrow \sigma^*_{C—H}$ interaction and approximately twice this value if the attacked carbon atom is substituted by two fluorine atoms. We think that the large differences of $\Delta(\Delta E_r)$ originate from this anomeric effect. The variations of $\Delta(\Delta E_r)$ are almost the same for the two radicals; thus, the choice of OMe as a model of OtBu is justified.

Reliability of Results

On the ground of previous experience, all the geometry optimizations were done at the B3LYP/6-31G(d) level. However, the barrier heights and binding energies of prereaction complexes differ from the results of single point calculations at higher levels of theory by factors of 3–6. This prompted us to investigate in deeper detail the reliability of different levels of geometry optimization using the system $OCH_3 + H_2C{=}CF_2$ as a benchmark. The most significant geometrical parameters are collected in Table VIII and the corresponding energetics are in Table IX.

The results reported in the tables show that the computational level chosen for geometry optimization has a small effect on the relative energies of stationary points, despite some quite large differences, especially for the structure of the intermediates. It is also reassuring that, as already found for similar reactions,[15] the basis set superposition error is very small at the B3LYP/6-311+G(2d,2p) level and its addition to B3LYP/6-31G(d) results leads to much improved values (see Table IX). Another possible source of error is the spin contamination of unrestricted computations. This problem was solved by using projection techniques at the MP2 level (PMP2) whereas the effect should be negligible in DFT computations in view of the very small deviation between the correct value of S^2 (0.75) and the values computed from the KS orbitals ($0.75 < S^2 < 0.755$ for prereaction complexes and products and $0.75 < S^2 < 0.755$ for transition structures).

It is remarkable that extension of the basis set has the same effect at the PMP2 and QCISD(T) level (see Table IX), and this confirms the reliability of composite procedures for the evaluation of thermodynamic and kinetic parameters in radical addition reactions.[10] From another point of view, it was recently suggested that for some open-shell systems QCISD(T) results could be less reliable than complete coupled cluster computations [CCSD(T)]. Our results show that both kinds of computations are comparable except for prereaction complexes. However, although quantitative thermodynamic and kinetic parameters can probably be obtained only by coupled cluster computations or using refined composite procedures,[10] relative values for differ-

TABLE VII.
Reaction Energies ΔE_r and Enthalpies ΔH_r (in kJ mol^{-1}) of Alkoxy Radical Addition to Fluoroethenes.

	OMe					
Level	**CH_2**CHF	CH_2**CHF**	**CH_2**CF_2	CH_2**CF_2**	**CHF**CF_2	CHF**CF_2**
ΔE_r [B3LYP/6-31G(d)]	−84.9	−112.5 (−27.6)	−91.3	−145.7 (−54.4)	−150.6	−176.2 (−25.6)
ΔE_r [B3LYP/6-311+G(2d,2p)]	−66.0	−97.5 (−31.5)	−74.4	−128.3 (−53.9)	−132.7	−155.8 (−23.1)
ΔE_r [PMP2/6-31G(d)]	−109.5	−148.2 (−38.7)	−118.0	−189.7 (−71.7)	−188.0	−219.6 (−31.6)
ΔE_r [PMP2/6-311+G(2d,2p)]	−105.6	−144.7 (−39.1)	−113.3	−181.0 (−67.7)	−181.2	−209.6 (−28.4)
ΔH_r	−71.2	−101.1 (−29.9)	−76.0	−137.0 (−61.0)	−136.8	−169.5 (−32.7)
	OtBu					
Level	**CH_2**CHF	CH_2**CHF**	**CH_2**CF_2	CH_2**CF_2**	**CHF**CF_2	CHF**CF_2**
ΔE_r [B3LYP/6-31G(d)]	−68.7	−88.0 (−19.3)	−76.1	−132.0 (−55.9)	−128.2	−158.0 (−29.8)
ΔE_r [B3LYP/6-311+G(d,p)]	−46.0	−67.2 (−21.2)	−54.7	−109.5 (−54.8)	−104.9	−139.1 (−34.2)
ΔE_r [PMP2/6-31G(d)]	−103.8	−113.2 (−29.4)	−113.2	−184.2 (−71.0)	−179.7	−211.3 (−31.6)
ΔE_r [PMP2/6-311+G(d,p)]	−99.3	−126.9 (−27.6)	−105.7	−170.2 (−64.5)	−169.9	−205.1 (−37.2)
ΔH_r	−57.2	−79.9 (−22.7)	−68.7	−127.8 (−59.1)	−115.1	−157.0 (−35.9)

Values in parentheses are the differences between the reaction energies or enthalpies of anomalous and regular pathways.

TABLE VIII.
Main Geometrical Parameters Optimized at Different Computational Levels for Addition of OCH_3 to $H_2C{=}CF_2$.

Parameter	B3LYP/6-31G(d)	B3LYP/6-311+G(2d,2p)	UMP2/6-31G(d)
		C	
O···C1	2.584	3.107	2.944
O···C2	2.906	3.414	3.461
		TS_r	
O···C2	2.039	2.011	1.966
∠OC2C1	103.7	105.7	104.5
H···F	2.758	2.905	2.697
		TS_a	
O···C1	2.074	2.041	1.967
∠OC1C2	94.0	94.5	92.6
H···F	2.473	2.537	2.830
		P_r	
O···C2	1.420	1.419	1.418
∠OC2C1	114.4	114.6	113.4
H···F	2.478	2.558	2.484
		P_a	
O···C1	1.360	1.352	1.361
∠OC1C2	110.4	111.1	110.2
H···F	2.488	2.499	2.462

The substituted carbon atom is labeled 1 and the unsubstituted carbon atom is labeled 2; the subscripts r and a refer to regular and anomalous pathways, respectively.

TABLE IX.

Energies of Different Stationary Points on Potential Energy Surface Governing Addition of OCH_3 to $H_2C{=}CF_2$ (kJ mol^{-1} with Respect to Reactants) Obtained by Different Methods and Basis Sets.

Geometry	Energy	C	TS_r	TS_a	P_r	P_a
B3LYP/6-31G(d)	B3LYP/6-31G(d)	−8.2	5.4	0.4	−91.3	−145.7
B3LYP/6-31G(d)	B3LYP/6-31G(d) + BSSE	1.6	18.0	13.9		
B3LYP/6-31G(d)	B3LYP/6-311+G(2d,2p)	−1.2	13.9	12.0	−74.4	−128.3
B3LYP/6-311+G(2d,2p)	B3LYP/6-311+G(2d,2p)	−1.8	13.4	12.4	−74.3	−128.1
B3LYP/6-311+G(2d,2p)	B3LYP/6-311+G(2d,2p) + BSSE	0.6	16.4	14.1		
B3LYP/6-31G(d)	PMP2/6-31G(d)	−9.4	15.1	10.3	−118.0	−189.7
B3LYP/6-31G(d)	PMP2/6-311+G(d,p)	−8.4	13.5	10.4	−118.0	−189.0
UMP2/6-31G(d)	PMP2/6-31G(d)	−9.1	14.6	9.7	−113.9	−181.0
UMP2/6-31G(d)	PMP2/6-311+G(d,p)	−7.9	16.1	13.0	−113.1	−179.3
		(1.2)	(1.5)	(3.3)	(0.8)	(1.7)
UMP2/6-31G(d)	QCISD(T)/6-31G(d)	−5.8	25.2	18.7	−96.3	−163.5
UMP2/6-31G(d)	QCISD(T)/6-311+G(d,p)	−4.6	26.7	22.0	−96.1	−161.8
		(1.2)	(1.5)	(3.3)	(0.2)	(1.7)
UMP2/6-31G(d)	CCSD(T)/6-31G(d)	−9.2	26.3	20.0	−95.7	−163.3
UMP2/6-31G(d)	CCSD(T)/6-311+G(d,p)[a]	−8.0	27.8	23.3	−95.5	−165.0

The variations related to basis set extension are given in parentheses.

[a] Estimated from CCSD(T)/6-31G(d) + QCISD(T)/6-311+G(d,p) − QCISD(T)/6-31G(d).

ent sites of the attack (i.e., the regioselectivity of the reaction) are also well reproduced by all methods from a quantitative point of view. Because this was the main concern of the present study, we use our standard level of computation in the discussion of the next section.

FACTORS RESPONSIBLE FOR REGIOSELECTIVITY

Besides the strength of the forming bond, Shaik and Canadell, using an SCD model, emphasized the role played by the spin densities of the attacked centers in the $^3\pi\pi^*$ states of different alkenes in determining the regiochemistry of radical additions to unsaturated bonds[31]: the preferred site of attack is the atom that possesses the highest spin density. The spin densities in the $^3\pi\pi^*$ states of fluoroethenes were calculated at various levels of theory[20]: all the calculations indicate a larger spin density on the CH_2 moiety of CH_2CHF and CH_2CF_2 and on the CF_2 moiety of $CHFCF_2$. Thus, as concerns this last substrate, the regiochemistry of the alkoxy addition is easily explained in the framework of the simplified SCD model because spin density and reaction enthalpy both favor the addition on the CF_2 end of trifluoroethene (see Fig. 7a).[32, 33]

It is well established that the methyl radical is less regiospecific than the OtBu radical toward trifluoroethene [$k_a/k_r = 2.1$ (Me) and 4.5 (OtBu)]: the large difference of $\Delta(\Delta E_r)$ [≈30 kJ mol^{-1} (OtBu), ≈−11 kJ mol^{-1} (Me)] is in line with the larger regioselectivity of OtBu. In the same way, the calculated intermolecular O···C distances in the TS agree with this scheme if we assume that the TS is very close to the crossing point of reactant and product configurations.

The preferential attack of alkoxy radicals occurs on the unsubstituted carbon atom of CH_2CHF; the spin density factor favors the addition on the CH_2 end (H_2C, 1.1101; FHC, 0.9468 at the B3LYP/6-31G* level) while the thermodynamic factor (energy difference = −19.3 kJ mol^{-1}) has an opposite effect.

The anomalous pathway is also preferred for alkoxy addition to CH_2CF_2; this substrate is characterized by the largest difference of spin densities (H_2C, 1.1117; F_2C, 0.8369 at the B3LYP/6-31G* level) and of reaction energies (−55.9 kJ mol^{-1}). The thermodynamic factor prevails over the spin density one. The qualitative correlation diagram reported in Figure 7b summarizes this regioselectivity.

In order to better assess the importance of this factor, as well as the polarity of the incoming radical, we considered the addition of some other radicals to CH_2CF_2. The results are summarized in Table X. The reasons for our choices are the following:

1. CH_3 was selected because it does not exhibit any polar character,[18, 34] and it gives an un-

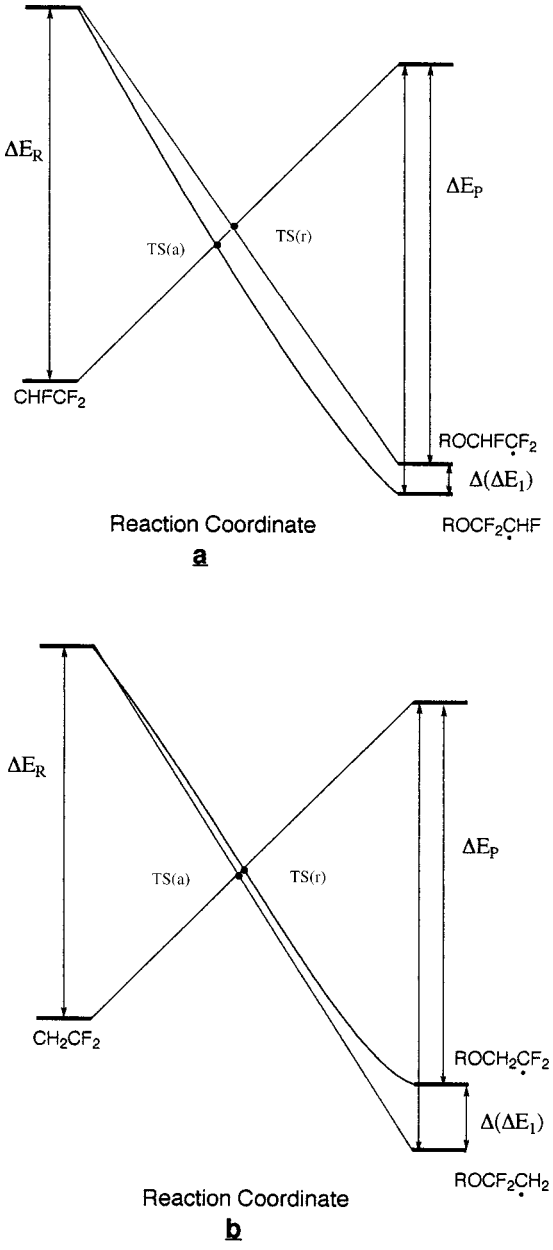

FIGURE 7. State correlation diagrams.

symmetrical fluorine substitution effect favoring anomalous addition[35];

2. CF_3 was chosen because it has an electrophilic character,[36] and it gives an unsymmetrical fluorine substitution effect favoring regular addition;
3. CH_2CN and CH_2OH were selected because they act as an electrophile[34b, 37] and nucleophile,[34b, 38] respectively, and do not give an unsymmetrical fluorine substitution effect.

The polar character of the radical, as well as the relative importance of charge transfer contributions to the ground-state wave function, may be assessed from the computed charge distribution (natural population analysis, NPA) within the TS for radical addition. According to the SCD model,[39] the principal valence-bond configurations that contribute to the TS ground-state wave function are[34b] (*R*, radical, *S*, substrate):

$$\mathrm{TS} = RS \leftrightarrow R^3S^* \leftrightarrow R^+S^-$$

if *R* acts as a donor in the *R*–*S* system (*R* nucleophilic radical), and

$$\mathrm{TS} = RS \leftrightarrow R^3S^* \leftrightarrow R^-S^+$$

if *R* acts as an acceptor in the *R*–*S* system (*R* electrophilic radical). On the basis of natural population analysis, CF_3, CH_2CN, OMe, and OtBu display an electrophilic behavior in the order OtBu $\approx$ OMe > CH_2CN > CF_3 while CH_2OH is nucleophilic toward CH_2CF_2.

Let us first comment on the results obtained for electrophilic radicals. The role of the thermodynamic factor in determining the regioselectivity of radical addition reactions is now emphasized: when the thermodynamic factor acts in the same direction [$\Delta(\Delta E_r) > 0$] as the spin density factor, the regular pathway is plainly preferred (entries 2 and 5 in Table X); if the two factors act in opposite directions, the anomalous pathway is slightly preferred if $\Delta(\Delta E_r)$ is very negative. However, a detailed comparison of the results (entries 2 and 5 in Table X) shows that the largest $\Delta(\Delta E^{\neq})$ value does not correspond necessarily to the most positive $\Delta(\Delta E_r)$ value. As a matter of fact, the difference $\Delta(\Delta E^{\neq})$ depends also on the location of the TSs along the reaction path, an earlier TS corresponding to a lower $\Delta(\Delta E^{\neq})$ (see Fig. 7); now CF_3 addition is more exothermic than the CH_2CN one and TSs with CF_3 are reached for larger intermolecular distances.

The results obtained for the addition of the nucleophilic radical CH_2OH are more surprising. B3LYP/6-31G(d) and PMP2/6-31G(d)//B3LYP/6-31G(d) results suggest a preferential addition on the substituted carbon atom, although the exothermicity of regular and anomalous pathways are very close (compare entries 1 and 6 of Table X). These trends cannot be rationalized by the simple SCD model. Close examination of $q(R)$ values shows a different behavior for electrophilic and nucleophilic radicals: invariably, in the former case the largest charge transfer in the TS is obtained for the addition on the CH_2 end; thus, a larger participation

TABLE X.

Energy Barriers, $\Delta E^{\neq}$, Reaction Energies, ΔE_r, Intermolecular O···C_{att} Distances, R, and Charge Transfer, $q(R)$, Related to Addition of Various Radicals to CH_2CF_2.

	$\Delta E^{\neq}$		ΔE_r		R		$q(R)$	
Radical R	**CH_2**CF_2	CH_2**CF_2**	**CH_2**CF_2	CH_2**CF_2**	**CH_2**CF_2	CH_2**CF_2**	**CH_2**CF_2	CH_2**CF_2**
CH_3	21.2	29.3 (8.1)	−138.4	−137.5 (0.9)	2.344	2.281	−0.025	0.002
	29.5	*33.0* (*3.2*)	*−144.2*	*−152.5* (*−8.3*)				
CF_3	5.6	15.4 (9.8)	−150.0	−125.6 (25.4)	2.423	2.316	−0.048	−0.019
	10.4	*15.7* (*5.3*)	*−168.9*	*−151.9* (*17.0*)				
OMe	5.4	0.4 (−5.0)	−91.3	−145.7 (−54.4)	2.039	2.074	−0.198	−0.161
	15.1	*10.3* (*−4.8*)	*−118.0*	*−189.7* (*−71.7*)				
OtBu	13.5	10.6 (−2.9)	−76.1	−132.0 (−55.9)	1.995	2.014	−0.201	−0.164
	12.5	*10.7* (*−1.8*)	*−113.2*	*−184.2* (*−71.0*)				
CH_2CN	27.2	45.3 (18.1)	−82.1	−70.1 (12.0)	2.231	2.199	−0.108	−0.088
	25.5	*34.4* (*8.9*)	*−112.2*	*−111.8* (*0.4*)				
CH_2OH	25.8	21.5 (−4.3)	−107.6	−108.4 (−0.8)	2.301	2.258	0.041	0.080
	29.7	*23.1* (*−6.6*)	*−125.4*	*−134.0* (*−8.6*)				

The values in parentheses are the differences $\Delta(\Delta E) = \Delta E(a) - \Delta E(r)$; energies are in kilojoules per mole, and distances are in angstroms.
The PMP2/6-31G(d) results are in italic.

of the R^-S^+ charge transfer configuration to the stabilization of the TS ground state is expected for the regular pathway. On the contrary, an opposite trend is found in the second case and the R^+S^- charge transfer configuration mixing in the TS is more effective for the anomalous pathway. A more complete curve-crossing diagram including RS, R^3S^* and R^+S^-, or R^-S^+ would be necessary to account for the regioselectivity. To the best of our knowledge, experimental and theoretical works devoted to systematic studies of polar effects on the regiochemistry of radical additions are very scarce. Further investigations in this direction would be valuable.

Conclusion

In this article we reported a comprehensive study of the addition of oxygen centered radicals to substituted ethenes by different quantum mechanical approaches. From a methodological point of view, B3LYP computations provide correct general trends whereas quantitative results can be obtained by single point post-HF computations at B3LYP geometries. Then the role of different factors in determining the regioselectivity of the reaction were analyzed in detail using SCDs. Our results can be summarized as follows:

- Oxygen centered radicals invariably form weak associations with substituted ethenes at long distance, but these adducts do not play a significant role in determining the regioselectivity.
- Hydrogen atoms of the OtBu radical form weak hydrogen bonds with ethene fluorines, but this interaction also has a negligible effect on the regioselectivity of the addition, which is, in fact, very similar for OtBu and OMe.
- The determining role of the thermodynamic effect in the orientation of the reaction is confirmed: the preferential addition of alkoxy radicals on the more substituted ends of di- and trifluoroethene is related to the larger stability of the product radicals ($ROCF_2CH_2$ and $ROCF_2CHF$). This is due, in turn, to an anomeric effect, which we analyzed in detail.
- A comparative study of the addition to difluoroethene of radicals showing different polarities pointed out the role of the polar factor in determining the preferential orientation of the reaction.

Acknowledgment

The first author gratefully acknowledges the CNUSC for the computer facilities.

References

1. Tedder, J. M. Angew Chen Int Ed Engl 1982, 21, 401.
2. Giese, B. Angew Chen Int Ed Engl 1983, 221, 753.
3. Fischer, H. In Free Radicals in Biology and the Environment; Minisci, F., Ed.; Kluwer: Dordrecht, 1997; p. 69.
4. Jones, M. J.; Moad, G.; Rizzardo, E.; Solomon, D. H. J Org Chem 1989, 54, 1607.
5. (a) Sosa, C.; Schlegel, H. B. J Am Chem Soc 1987, 109, 4193; (b) Sosa, C.; Schlegel, H. B. J Am Chem Soc 1987, 109, 7007.
6. Donovan, W. H.; Famini, G. R. J Phys Chem 1994, 98, 7811.
7. Alvarez–Idaboy, J. R.; Diaz–Acosta, I.; Vivier–Bunge, A. J Comput Chem 1998, 19, 811.
8. Sekusàck, S.; Liedl, K. R.; Sabljic, A. J Phys Chem A 1998, 102, 1583.
9. Arnaud, R. New J Chem 1991, 15, 615.
10. For an assessment of theoretical procedures for the calculation of activation barriers and thermochemistry, see (a) Wong, M. W.; Radom, L. J Phys Chem 1998, 102, 2237; (b) Mayer, P. M.; Parkinson, C. J.; Smith, D. M.; Radom, L. J Chem Phys 1998, 108, 604.
11. Parr, R. G.; Yang, W. J. Density-Functional Theory of Atoms and Molecules; Oxford University Press: New York, 1989.
12. Lee, C.; Yang, W.; Parr, R. G. Phys Rev Sect B 1988, 37, 785.
13. Becke, A. D. J Chem Phys 1993, 98, 5648.
14. Barone, V. In Advances in Density Functional Methods, Part I; Chong, D. P., Ed.; World Scientific: Singapore, 1996; p. 278.
15. Barone, V.; Orlandini, L. Chem Phys Lett 1995, 246, 45.
16. Bottoni, A. J Chem Soc Perkin Trans 2 1996, 2041.
17. Jursic, B. S. J Chem Soc Perkin Trans 2 1997, 637.
18. Arnaud, R.; Bugaud, N.; Vetere, V.; Barone, V. J Am Chem Soc 1998, 120, 5733.
19. (a) Korchowi, J.; Uchimaru, T. J Phys Chem A 1998, 102, 2439; (b) Korchowi, J.; Uchimaru, T. J Phys Chem A 1998, 102, 6682.
20. Arnaud, R.; Vetere, V.; Barone, V. Chem Phys Lett 1998, 2936, 295.
21. Frisch, M. J.; Trucks, G. W.; Schlegel, H. B.; Scuseria, G. E.; Robb, M. A.; Cheeseman, J. R.; Zakrzewski, V. G.; Montgomery, J. A.; Stratmann, R. E.; Burant, J. C.; Dapprich, S.; Millam, J. M.; Daniels, A. D.; Kudin, K. N.; Strain, M. C.; Farkas, O.; Tomasi, J.; Barone, V.; Cossi, M.; Cammi, R.; Mennucci, B.; Pomelli, C.; Adamo, C.; Clifford, S.; Ochterski, J.; Petersson, G. A.; Ayala, P. Y.; Cui, Q.; Morokuma, K.; Malick, D. K.; Rabuck, A. D.; Raghavachari, K.; Foresman, J. B.; Cioslowski, J.; Ortiz, J. V.; Stefanov, B. B.; Liu, G.; Liashenko, A.; Piskorz, P.; Komaromi, I.; Gomperts, R.; Martin, R. L.; Fox, D. J.; Keith, T.; Al-Laham, M. A.; Peng, C. Y.; Nanayakkara, A.; Gonzalez, C.; Challacombe, M.; Gill, P. M. W.; Johnson, B.; Chen, W.; Wong, M. W.; Andres, J. L.; Head–Gordon, M.; Replogle, E. S.; Pople, J. A. Gaussian 98, Revision A.6; Gaussian, Inc.: Pittsburgh, PA, 1998.
22. Descriptions of the basis set and an explanation of standard levels of theory can be found in the following: Foresman, J. B.; Frisch, A. E. Exploring Chemistry with Electronic Structure Methods, 2nd ed.; Gaussian, Inc.: Pittsburgh, PA, 1996.
23. Gonzalez, C.; Schlegel, H. B. J Phys Chem 1990, 94, 5523.
24. Eyring, H.; Lin, S. H.; Lin, S. M. Basic Chemical Kinetics; Wiley: New York, 1980.
25. (a) Curtiss, L. A.; Pochatko, D. J.; Reed, A. E.; Weinhold, F. J Chem Phys 1983, 82, 2679; (b) Reed, A. E.; Curtiss, L. A.; Weinhold, F. Chem Rev 1988, 88, 899.
26. Tyrell, J.; Weinstock, R. B.; Weinhold, F. Int J Quantum Chem 1981, 19, 781.
27. Bader, R. F. W. Atoms in Molecules. A Quantum Theory; Oxford University Press: Oxford, U.K., 1990.
28. For a recent review of weak hydrogen bonds see: Alkorta, I.; Rozas, I.; Elguero, J. Chem Soc Rev 1998, 27, 163.
29. (a) Mo, O.; Yanez, M.; Elguero, J. J Chem Phys 1992, 97, 6628; (b) Kock, U.; Popelier, P. L. A. J Phys Chem 1995, 99, 9747; (c) Alkorta, I.; Elguero, J. J Phys Chem 1996, 100, 19367.
30. Arnaud, R. J Comput Chem 1994, 15, 1341.
31. Shaik, S. S.; Canadell, E. J Am Chem Soc 1990, 112, 1446.
32. The assumptions to build up the correlation diagram depicted in Figure 7 are identical to those used by Bottoni in his study of addition of silyl radical to ethene and propene;[33] ΔE_R is taken equal to the vertical $\pi \rightarrow \pi^*$ triplet excitation of CH_2CF_2; in our case, ΔE_P which corresponds to the coupling/decoupling between the two electrons in the new O—C bond cannot be considered identical for the two directions of attack. Insofar as ΔE_P is related to the O—C bond energies, we assume that $\Delta E_P + \Delta E_r$ is almost the same for the two directions. In order to introduce the difference in the spin density of the two carbon centers, a curved line is used to translate the larger spin coupling.
33. Bottoni, A. J Phys Chem A 1997, 101, 4402.
34. (a) Wong, M. W.; Pross, A.; Radom, L. J Am Chem Soc 1993, 115, 11050; (b) Wong, M. W.; Pross, A.; Radom, L. J Am Chem Soc 1994, 116, 6284.
35. Epiotis, N. D.; Cherry, W. R.; Shaik, S. S.; Yates, R. L.; Bernardi, F. Topics Curr Chem 1977, 70, 199.
36. Dolbier, W. R., Jr. Chem Rev 1996, 96, 1557.
37. Wu, J. Q.; Beranek, I.; Fischer, H. Helv Chim Acta 1995, 78, 194.
38. Wu, J. Q.; Fischer, H. Int J Chem Kinet 1995, 327, 167.
39. Shaik, S. S.; Ioffe, A.; Reddy, A. C.; Pross, A. J Am Chem Soc 1994, 116, 262.